

Green Synthesis of Zinc Oxide (ZnO) Nanoparticles Using Kepok Banana Leaf Extract (*Musa Paradisiaca* L.) for Methylene Blue Degradation

Amrina Mustaqim^{1*}, Vera Khoirunisa¹, Syamsyarief Baqaruzi², Nadia Soni Utami¹, Retno Maharsi³

¹ Engineering Physics Department, Faculty of Industrial Technology, Institut Teknologi Sumatera, Indonesia

² Electrical Engineering Department, Faculty of Industrial Technology, Institut Teknologi Sumatera, Indonesia

³ Biomedical Engineering Department, Faculty of Industrial Technology, Institut Teknologi Sumatera, Indonesia

Corresponding Authors E-mail: amrina.mustaqim@tf.itera.ac.id

Article Info

Article info:

Received: 23-10-2025

Revised: 10-05-2026

Accepted: 12-05-2026

Keywords:

ZnO; Banana Leaf; Green Synthesis; Methylene Blue; Photocatalysis

How To Cite:

A. Mustaqim, V. Khoirunisa, S. Baqaruzi, N. S. Utami, R. Maharsi "Green Synthesis of Zinc Oxide (ZnO) Nanoparticles Using Kepok Banana Leaf Extract (*Musa Paradisiaca* L.) for Methylene Blue Degradation", *Indonesian Physical Review*, vol. 9, no. 2, p 329-344, 2026.

DOI:

<https://doi.org/10.29303/ipr.v9i2.614>

Abstract

This study examines the effect of *Musa paradisiaca* L. leaf extract concentration (6%, 8%, and 10%) on the structural, morphological, and photocatalytic properties of ZnO nanoparticles synthesized via a green method, with a focus on methylene blue (MB) degradation. XRD analysis confirms the formation of ZnO with crystallite sizes in the range of 34–37 nm, while SEM observations show particle sizes of approximately 40–130 nm, indicating agglomeration. The results also show that increasing the extract concentration from 6% to 10% reduces the band gap energy from 3.24 eV to 3.05 eV, which is followed by an increase in MB degradation efficiency up to 78% after 180 minutes. This trend indicates a clear relationship between extract concentration, band gap energy, and photocatalytic activity, where a lower band gap enables more effective light absorption and enhances degradation performance. Overall, the findings demonstrate that extract concentration is a key parameter in improving the photocatalytic performance of ZnO nanoparticles for dye degradation.



Copyright (c) 2026 by Author(s). This work is licensed under a Creative Commons Attribution-ShareAlike 4.0 International License.

Introduction

Industrial development in Indonesia has experienced rapid and significant growth in recent years. However, this progress is often accompanied by environmental challenges, particularly water pollution resulting from industrial effluents [1-3]. Various industrial sectors, including plastics, paints, food processing, cosmetics, and textiles, contribute to the discharge of

hazardous waste into aquatic environments [4,5]. Among these, the textile industry is recognized as a major source of water pollution due to the presence of synthetic dyes, such as Rhodamine B, Victoria blue, Eriochrome, Black-T (EBT), Thymol blue, and Methylene Blue (MB) [6-11].

Methylene blue (MB) has received particular attention due to its widespread use and persistence in aquatic environments. This dye exhibits high chemical stability and resistance to natural degradation, leading to its accumulation in water bodies. Prolonged exposure to MB can pose serious environmental and health risks, including toxicity to aquatic organisms. More concerningly, it has a high potential for adverse effects on human health, such as skin irritation, respiratory problems, and possible mutagenic or carcinogenic impacts [12].

Various treatment methods have been developed to remove dye pollutants from wastewater, including adsorption, coagulation-flocculation, membrane filtration, and biological degradation processes [13,14]. Adsorption is widely applied due to its simplicity and effectiveness; however, it only transfers pollutants from the liquid phase to a solid phase, requiring further regeneration or disposal [15]. Biological methods are considered environmentally friendly, but are often limited by the low biodegradability and toxicity of synthetic dyes such as MB [12,16]. Meanwhile, advanced separation techniques such as membrane filtration offer high removal efficiency but suffer from drawbacks, including membrane fouling and high operational costs [2,13]. Among these approaches, photocatalysis has emerged as one of the most promising methods due to its ability to completely mineralize organic pollutants into harmless end products such as CO_2 and H_2O under light irradiation [16, 17].

In particular, semiconductor-based photocatalysts have attracted significant attention due to their superior performance compared to conventional treatment methods for dye degradation. Various semiconductor materials have been extensively investigated as photocatalysts for dye degradation, including titanium dioxide (TiO_2), zinc oxide (ZnO), cadmium sulfide (CdS), tungsten trioxide (WO_3), and iron(III) oxide (Fe_2O_3) [18]. TiO_2 is widely studied due to its strong oxidative ability and stability; however, its wide band gap limits activity to UV light [16]. CdS shows good visible-light absorption but suffers from photocorrosion and toxicity issues, while WO_3 and Fe_2O_3 enable visible-light activation but exhibit lower efficiency due to rapid electron-hole recombination [19]. In contrast, zinc oxide (ZnO) offers band gap comparable to TiO_2 with higher electron mobility, along with low cost, abundance, non-toxicity, and environmental friendliness, making it a promising photocatalyst for degrading MB [18].

To further enhance the sustainability of ZnO production, green synthesis approaches have been increasingly explored as alternatives to conventional chemical methods [20]. Traditional synthesis route, including sol-gel, hydrothermal, precipitation, and chemical vapor deposition methods, often require high temperatures, toxic chemicals, and complex processing conditions, leading to high energy consumption and potential environmental hazards. In contrast, green synthesis utilizes plant extracts as natural reducing and stabilizing agents, offering a simpler, cost-effective, and environmentally benign process. Biomolecules such as flavonoids, phenolic compounds, and proteins present in plant extracts play a crucial role in controlling nucleation, growth, and stabilization of ZnO nanoparticles. These compounds can influence particle size, morphology, and defect formation, which are key factors governing photocatalytic performance [21-23].

Several studies have reported the green synthesis using various plant extracts, such as widow flower (*Calotropis gigantea*) [24], papaya fruit (*Carica Papaya*) [25], aloe vera (*Aloe barbadensis Miller*) [26], black nightshade fruit (*Solanum nigrum*) [27], pomegranate fruit (*Punica granatum*) [28], moringa leaves (*Moringa oleifera*) [29] and basil leaves (*Ocimum* sp.) [30]. These methods were successfully employed for ZnO synthesis. However, the synthesis using those various plants as the agents still has some limitations, including relatively large particle size, high agglomeration, unstable phytochemical composition, and the need for specific synthesis conditions [24-26].

In contrast, the extract of kepok banana leaves (*Musa paradisiaca* L.) is reported to contain relatively stable flavonoid and phenolic compounds [31], is easy to process, non-mucilaginous, and has the potential to produce ZnO nanoparticles with improved dispersion and smaller particle size [26]. These phytochemicals can act as both reducing and capping agents through hydroxyl and carbonyl functional groups that interact with Zn^{2+} ions, thereby influencing nucleation, crystal growth, and defect formation during ZnO synthesis [32]. The abundance and low cost of this biomass further support its use as an environmentally friendly alternative.

Previous studies have demonstrated that banana-derived biomass, particularly banana peel, has been widely utilized in material synthesis and environmental applications. For instance, banana peel has been used in the synthesis of zinc oxide (ZnO)-based composites and bioplastics with antibacterial properties [33-35]. In addition, banana peel-derived materials have been applied as adsorbents and catalysts for dye removal, including the degradation of methylene blue (MB) through modified cellulose and heterogeneous Fenton processes [36]. These studies highlight the potential of banana biomass as a low-cost and sustainable resource for environmental remediation.

However, most existing works focus on banana peel rather than leaf extracts, and the applications are generally limited to adsorption, antibacterial activity, or catalysis assisted by additional metals (e.g., Fe). The use of kepok banana (*Musa paradisiaca* L.) leaf extract as a bioreducing and stabilizing agent in the green synthesis of ZnO nanoparticles, particularly for photocatalytic degradation of MB, remains largely unexplored. Therefore, this study aims to fill this gap by investigating the role of kepok banana leaf extract in controlling ZnO nanoparticle properties and evaluating its photocatalytic performance, offering a novel and sustainable approach for dye wastewater treatment.

In this study, the effect of varying the concentration of kepok banana (*Musa paradisiaca* L.) leaf extract (6%, 8%, and 10%) on the synthesis of ZnO nanoparticles was investigated. The selected concentration range was used to examine its influence on particle formation, particularly in terms of particle size, dispersion, and agglomeration behavior [37]. The synthesized ZnO nanoparticles were subsequently evaluated for their photocatalytic activity in degrading methylene blue (MB). Optical properties were analyzed using UV-Vis spectroscopy, while functional groups, crystal structure, crystallite size, and morphology were characterized using Fourier Transform Infrared Spectroscopy (FTIR), X-ray diffraction (XRD), and Field Emission Scanning Electron Microscopy (FESEM), respectively.

Experimental Method

The whole experimental procedure was illustrated in Figure 1. The materials used in this study included kepok banana leaves (*Musa paradisiaca* L.) collected from a local plantation in

Lampung Province, Indonesia; analytical-grade zinc acetate dihydrate ($\text{Zn}(\text{OAc})_2 \cdot 2\text{H}_2\text{O}$, Merck), sodium hydroxide (NaOH, Merck), distilled water and methylene blue.



Figure 1. Schematic diagram of the synthesis process of ZnO using kepok banana leaves extract.

The extract of kepok banana leaves was prepared from fresh leaves. The leaves were washed, dried in an oven at 100°C for 9 minutes, and then ground in a mortar. Extract solutions were prepared in three different concentrations (6%, 8%, and 10% b/v), calculated proportionally on 100 g of dried leaves. Each sample was dissolved in 100 mL of distilled water and heated at 80°C for 10 minutes using a hot plate with magnetic stirring. The solution was then cooled to room temperature, filtered using filter paper, and stored at 4°C for subsequent experiments.

In the synthesis of ZnO, three beakers were prepared, each containing 10 mL of kepok banana leaf extract at different concentrations. Each beaker was added with 50 mL of 0.1 M zinc acetate dihydrate [$\text{Zn}(\text{CH}_3\text{CO}_2)_2 \cdot 2\text{H}_2\text{O}$] solution, and the mixture was stirred using a hot plate stirrer at 350 rpm for 25 minutes at room temperature. Subsequently, 0.1 M NaOH solution was added slowly until the pH reached 12 to ensure complete precipitation of $\text{Zn}(\text{OH})_2$ precursors and to provide alkaline conditions favorable for the formation of highly crystalline ZnO [38], followed by continuous stirring for 3 hours until the solution color faded. The suspension was then allowed to settle for 24 hours. The resulting precipitate was collected by centrifugation at 4000 rpm for 20 minutes and then dried in an oven at 150°C for 3 hours to obtain a powder product. The final samples prepared using 6%, 8%, and 10% extract concentrations were denoted as ZnO-DP6 (6%), ZnO-DP8 (8%), and ZnO-DP10 (10%).

The resulting ZnO nanoparticles were then characterized using UV-Vis spectroscopy, Fourier Transform Infrared Spectroscopy (FTIR), X-ray diffraction (XRD), and Field Emission Scanning Electron Microscopy (FESEM) at the UPT Labororium Terpadu Institut Teknologi Sumatera and Badan Riset dan Inovasi Nasional (BRIN), Serpong Indoensia. UV-Vis spectrophotometer characterization was conducted to study the optical properties of ZnO nanoparticles, including band gap energy and photocatalytic activity during methylene blue (MB) degradation. Spectra were recorded in the range of 200-800 nm using Jeanway 6850 and Genesys 150 instruments [39]. FTIR analysis was performed to identify the functional groups associated with ZnO nanoparticles synthesized using kepok banana leaf extract. The spectra were measured in the range of $400\text{-}4000\text{ cm}^{-1}$ using an IRSpirit-T (SHIMADZU) spectrometer [40]. The structure and size of the synthesized ZnO crystals were examined using XRD (Multipurpose X-ray Diffraction System with Built-In Intelligent Guidance) with an analytical empirical powder diffractometer, using $\text{Cu K}\alpha$ radiation at a wavelength of 1.54184 \AA [41]. The crystal size (D) were calculated using Debye-Scherrer formula: $D = k\lambda/\beta\cos\theta$, where k is the Scherrer's constant (0.94), λ is the X-ray wavelength (1.5406 \AA), β is the peak width at half maximum (FWHM), and θ is the Bragg diffraction angle [42]. Particle morphology was

analyzed using FE-SEM, which allows observation of nanoscale structures with high spatial resolution [43].

Photocatalytic activity was evaluated using methylene blue (MB) solution with a final concentration of 10 ppm, prepared by diluting 3 mL of 100 ppm MB stock solution in 30 mL of distilled water. A total of 0.001 g of synthesized ZnO was mixed with MB solution and stirred using a magnetic stirrer at 300 rpm and hot plate. The solution was placed in a photocatalytic chamber and tested under two experimental conditions: (i) with 11 watts UV light exposure, and (ii) without UV light exposure, with samples taken at intervals of 0, 60, 120, and 180 minutes. The wavelength of UV lights were in a range of 280 – 315 nm. After each interval, the suspension was centrifuged to remove catalyst particles, and the supernatant was analyzed using a UV-Vis spectrophotometer to determine the residual MB concentration based on absorbance measurements. The percentage of MB degradation at each time interval was calculated based on Equation (1) [44].

$$h(\%) = \frac{C_0 - C_t}{C_0} \times 100\% \quad (1)$$

Where η (%) represents the percentage of degradation, C_0 represents the highest absorbance of methylene blue (MB) solution at time 0 minutes and C_t represents the highest absorbance of the solution at a certain time.

Result and Discussion

UV-Vis characterization

ZnO samples that have been mixed with kepok banana leaf extract are analyzed using a UV-Vis spectrophotometer, by observing the absorbance signal in the wavelength range of 300-400 nm. ZnO samples containing kepok banana leaf extract with variations of 6 g, 8 g, and 10 g were named ZnO-DP6, ZnO-DP8, and ZnO-DP10, respectively. The measurement results can be seen at Figure 2.

It can be observed that the ZnO-DP6, ZnO-DP8, and ZnO-DP10 samples show absorbance peaks at wavelengths of 342 nm, 320 nm, and 306 nm. These results are consistent with research conducted by Xiaodong Zhu (2021), which states that the formation of ZnO can be observed at wavelengths around 300 nm to 400 nm [45, 46]. The absorbance data of the ZnO samples obtained will be used to calculate the band gap energy of the synthesized ZnO nanoparticles, by applying the Tauc plot method [47, 48]. Equation (2) is used to calculate the band gap energy of the material [49].

$$\alpha h\nu = A (h\nu - E_g)^n \quad (2)$$

Where α is the absorbance coefficient, $h\nu$ is the photon energy (eV), E_g is the energy band gap (eV), A is a proportionality constant, and n is an exponent that depends on the type of electronic transition that occurs in the material. The energy band gap obtained using the above equation can be observed in Figure 3.

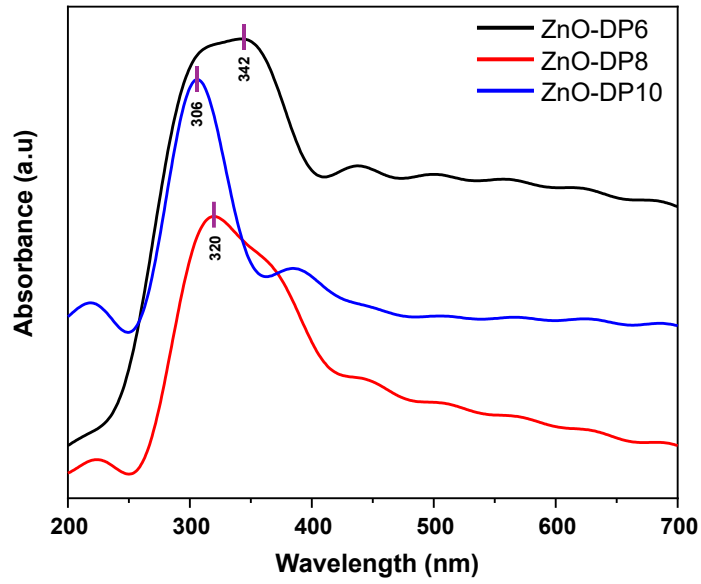


Figure 2. UV-visible spectra of ZnO samples with variations of kepok banana leaf extract

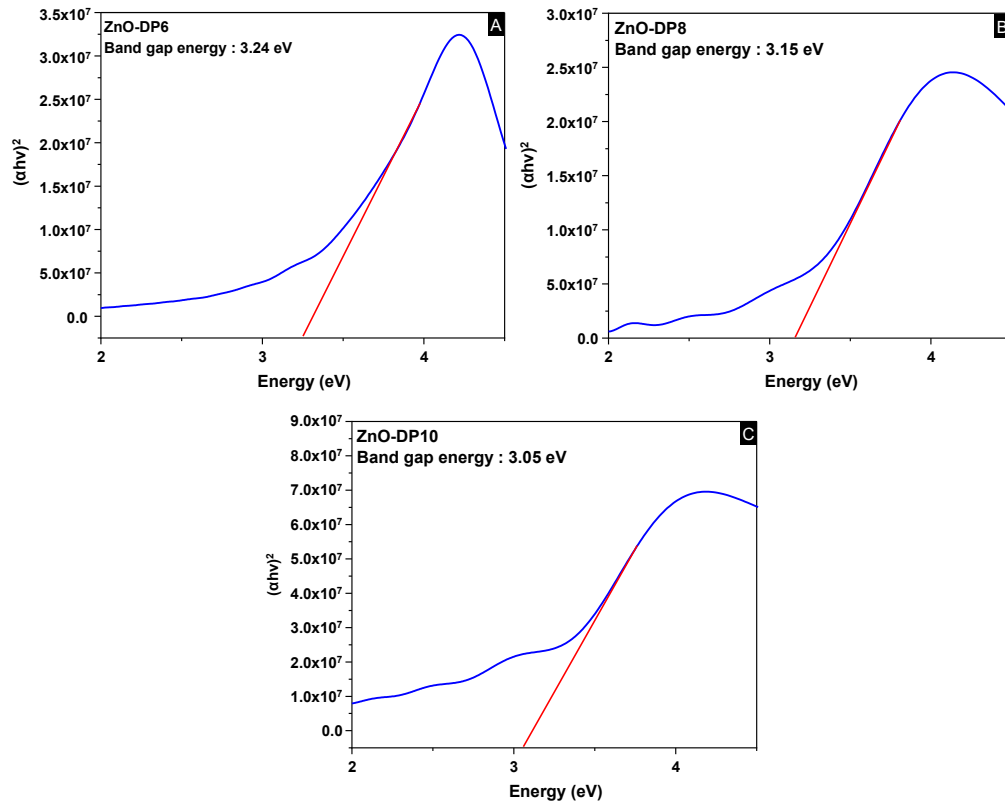


Figure 3. Optical band gap of ZnO samples (A) ZnO-DP6, (B) ZnO-DP8, and (C) ZnO-DP10

It can be seen that the energy band gap values obtained for ZnO-NPs (ZnO-DP6, ZnO-DP8, and ZnO-DP10) are 3.24, 3.15, and 3.05 eV, respectively with extract weight variations of 6, 8, and 10 g, which are close to the theoretical value of the energy band gap of about 3.37 eV [50]. These results show that increasing the volume of extract used tends to reduce the energy band gap of ZnO banana leaves [51]. This change in energy band gap is usually influenced by the structure, size, and shape of the nanoparticles, which can be affected by variations in extract volume [52].

FT-IR characterizations

FTIR analysis was performed to identify the functional groups on ZnO nanoparticles synthesized using kepok banana (*Musa Paradisiaca* L.) leaf extract. This process provides information regarding the molecules and biomolecules in the plant extract that play a role in the synthesis of nanoparticles. FTIR spectra were measured in the range of 4000 to 400 cm^{-1} , and the results can be observed in Figure 4.a. In the FTIR spectrum, significant absorbance peaks appeared at wave numbers 3737 cm^{-1} , 1630 cm^{-1} , 1494 cm^{-1} , 1405 cm^{-1} , 1057 cm^{-1} , 920 cm^{-1} , 680 cm^{-1} , and 450 cm^{-1} . The peak at 3737 cm^{-1} shows O-H bond stretching vibrations, which are related to free hydroxyl groups in phenolic compounds, derived from flavonoids in kepok banana leaves [53, 54]. The peak at 1630 cm^{-1} indicates the presence of alkene bonds (C=C), while the peaks at 1494 cm^{-1} and 1405 cm^{-1} indicate the presence of aromatic rings (C-C). The peak at 1057 cm^{-1} indicates bond stretching (C-C), and at 920 cm^{-1} is related to bond stretching (C-O)[54]. Functional groups such as O-H and C=C in kepok banana leaf extract act as effective reducing agents in the synthesis of ZnO nanoparticles [55].

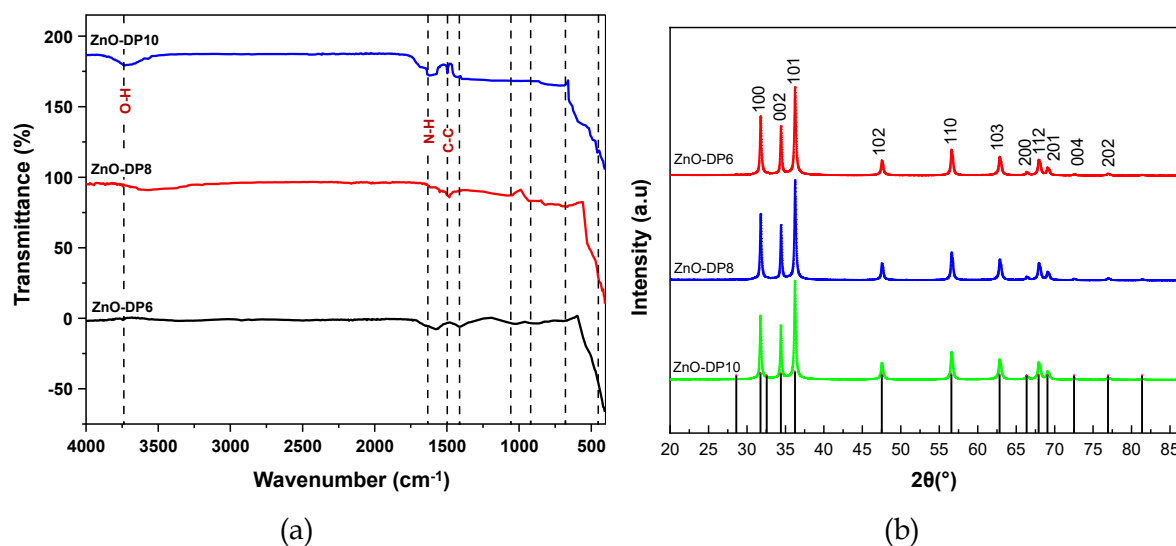


Figure 4. (a) FTIR spectra (b) XRD pattern of the ZnO samples

The characteristic peaks of ZnO nanoparticles are usually observed at wave numbers below 900 cm^{-1} . In this case, the absorption peaks at 680 cm^{-1} and 496 cm^{-1} indicate the formation of ZnO-NPs [56-58]. In the ZnO-DP10 sample, the peak at 496 cm^{-1} looks most dominant compared to the other peaks, indicating stronger ZnO formation [59].

X-ray Diffraction characterizations

X-ray Diffraction (XRD) is a technique used to obtain information about the size and structural characteristics of crystals. In this study, the XRD results show a diffractogram with 11 peaks that can be observed at various angles. Figure 3b shows the X-ray diffraction pattern of the synthesized ZnO nanoparticles, with peaks observed at angles of 31.75° , 34.4° , 36.23° , 47.54° , 56.59° , 62.85° , 66.42° , 67.94° , 69.11° , 72.57° , and 77.06° . These peaks correspond to the standard JCPDS File No. 00-036-1451, which shows a hexagonal wurtzite crystal structure.

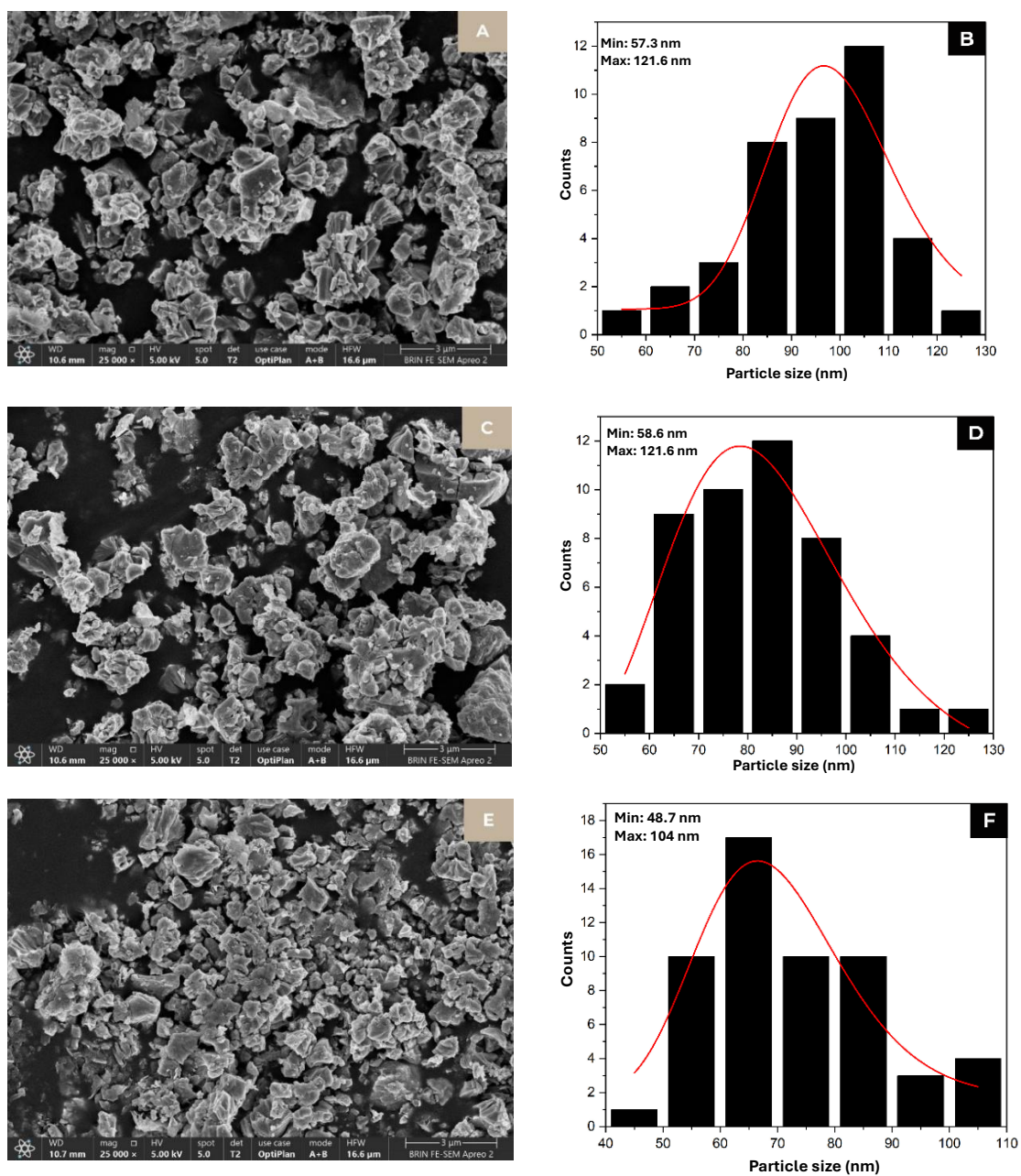


Figure 5. SEM images of synthesized ZnO ZnO-DP6 (A), ZnO-DP8 (C) and ZnO-DP10 (E). Particle size distribution of the ZnO-DP6 (B), ZnO-DP8 (D) and ZnO-DP10 (F)

The diffraction patterns observed at angles between 30° to 77° indicate a high degree of purity in the synthesized ZnO nanoparticles. All observed peaks show a match with the hexagonal wurtzite structure in accordance with JCPDS standard No. 36-1451. Figure 4b provides a clear visualization of the X-ray diffraction pattern. In addition, the XRD analysis results were also used to determine the crystal size of ZnO nanoparticles by applying the Debye-Scherrer equation. Based on this analysis, the crystal sizes obtained for ZnO-DP6, ZnO-DP8, and ZnO-DP10 samples are 34.95 nm, 37.29 nm, and 35.82 nm, respectively.

SEM characterizations

SEM images of ZnO synthesized using kepok banana leaf extract were recorded at various magnifications to get the morphology and particle size. This characterization provides information on the shape and size of ZnO produced with varying extract concentrations. The characterization results using Field Emission Scanning Electron Microscopy (FESEM) of ZnO samples synthesized with different extract concentrations are shown at Figure 5.

In the sample with 10% extract (ZnO-DP10), Figure 5 (E) shows the tendency of nanoparticle formation. The morphology of the particles was further examined using FESEM at 25,000x magnification, where the observed particles ranged in size from 40 to 130 nm. The ZnO was then analyzed using ImageJ software to determine the average particle size as well as the particle distribution by size, which can be seen in Figure 4 (B, D, F). The FESEM results indicate larger sizes than the XRD crystallite values, suggesting partial agglomeration of primary ZnO crystallites during particle growth. Moreover, the average particle size decreased with increasing extract concentration, indicating that the extract likely acted as a stabilizing agent that suppressed excessive grain growth and particle aggregation [60].

Photocatalytic degradations Studies

During the degradation process, there is a change in the color intensity of the MB solution, which can be observed through the measurement of absorbance values using a UV-Vis spectrophotometer. The maximum absorbance of MB was detected at a wavelength of 664 nm. Meanwhile, the MB solution that was not exposed to sunlight did not experience significant color change or degradation. The results of MB degradation accompanied by irradiation can be observed in Figure 6.

As seen in the spectrum, there is a gradual decrease in the peak intensity of methylene blue (MB) at a wavelength of 664 nm along with an increase in UV exposure time from 0 to 180 minutes. This decrease in intensity indicates that ZnO nanoparticles produced from kepok banana leaf extract can degrade methylene blue (MB) dye in solution. The efficiency of methylene blue (MB) degradation can be seen in Figure 7 which illustrates the comparison between light conditions (with UV irradiation) and dark conditions (without UV irradiation).

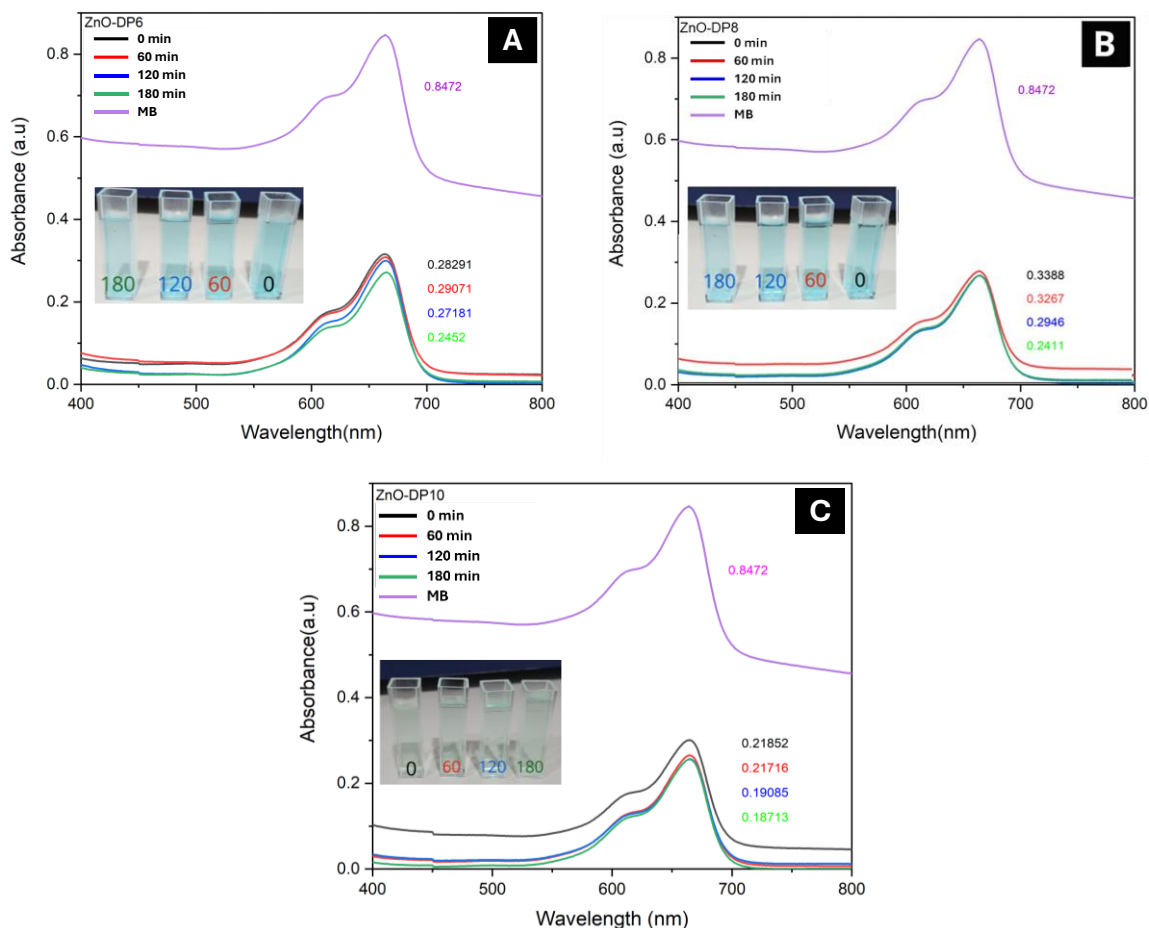


Figure 6. The absorbance spectra of Methylene Blue in 180 min (A) ZnO-DP6, (B) ZnO-DP8 and (C) ZnO-DP10

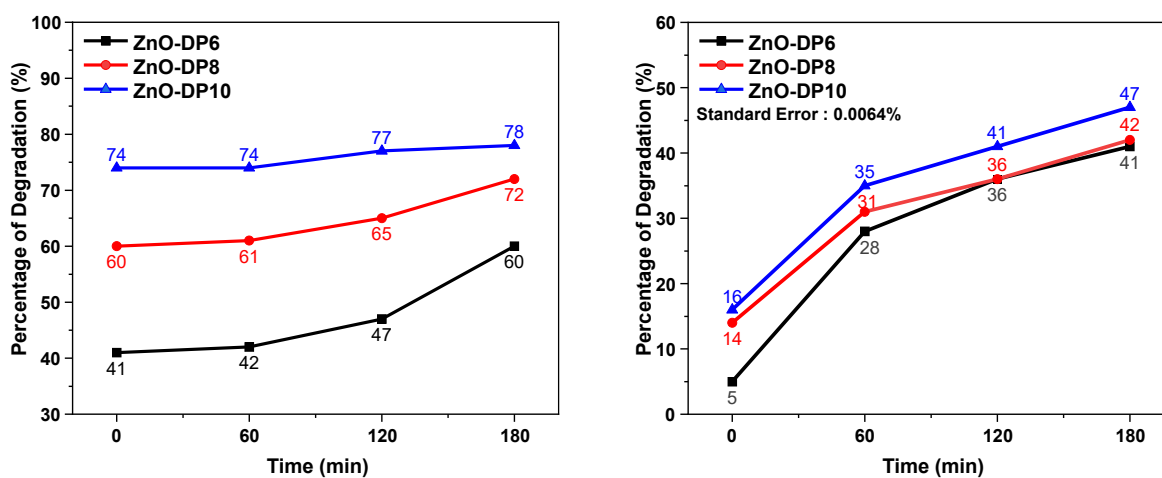


Figure 7. Comparison chart of degradation percentage in (A) light condition and (B) dark condition

The results of this study show that the addition of ZnO into methylene blue (MB) solution increases the degradation efficiency as the irradiation time increases. When ZnO was added,

the degradation process of methylene blue (MB) became more effective. However, under dark conditions, although there is an increase in degradation efficiency, the changes that occur are not very significant.

The FESEM results are consistent with the photocatalytic performance of the synthesized ZnO samples. As the extract concentration increased, the average particle size became smaller and particle agglomeration was reduced, indicating better dispersion of the ZnO particles. Smaller and less aggregated particles usually provide a larger active surface area and more available sites for interaction with methylene blue (MB) molecules during irradiation. This is in line with the photocatalytic results, where ZnO-DP10 showed the smallest particle size and achieved the highest degradation efficiency. In contrast, samples with larger and more agglomerated particles showed lower photocatalytic performance.

The photocatalytic degradation of methylene blue (MB) by zinc oxide (ZnO) under UV irradiation proceeds through the generation of electron-hole pairs after photon absorption with energy equal to or higher than the ZnO band gap. The photogenerated holes (h^+) react with H_2O or OH^- to form hydroxyl radicals ($\bullet OH$), while electrons reduce dissolved oxygen to generate superoxide radicals ($O_2\bullet^-$). These reactive species play an important role in oxidizing and decomposing MB molecules into smaller and less harmful products [61].

ZnO synthesized using kepok banana leaf extract (*Musa Paradisiaca L.*) showed the ability to degrade methylene blue (MB) with the highest efficiency reaching 78% after 180 minutes of irradiation. Several previous studies that also synthesized ZnO for photocatalyst applications using various synthesis methods showed similar results. The results of these studies can be seen in Table 1.

Table 1. Comparison of the results of the current research with previous research related to the synthesis of ZnO for MB degradation

No	Materials	Type of plant	Pollutant	Percentage Degradation	Time	Reference
1		<i>Brassica oleracea L.</i>	MB	74%	180 min	[62]
2	ZnO	-	MB	76%	180 min	[63]
3		<i>Musa Paradisiaca L.</i>	MB	78%	180 min	This Study

Table 1 compares the performance of the ZnO photocatalyst synthesized in this study with several previous plant-based ZnO materials for the degradation of methylene blue (MB). Under the same reaction time of 180 minutes, ZnO prepared using kepok banana (*Musa paradisiaca L.*) leaf extract showed the highest degradation efficiency of 78%, which is higher than those reported using *Brassica oleracea L.* (74%) [62]. This better performance may be related to the ability of the banana leaf extract to assist the formation of ZnO nanoparticles with improved dispersion and reduced agglomeration, leading to more active surface sites during the photocatalytic process. These results suggest that kepok banana leaf extract has strong potential as an eco-friendly and effective natural agent for synthesizing ZnO photocatalysts.

Conclusion

This study demonstrates that the concentration of *Musa paradisiaca* L. leaf extract plays an important role in determining the photocatalytic performance of ZnO nanoparticles. The results show that increasing the extract concentration from 6% to 10% leads to a decrease in band gap energy from 3.24 eV to 3.05 eV, which is followed by an increase in methylene blue (MB) degradation efficiency up to 78% after 180 minutes. This trend indicates a clear relationship between extract concentration, band gap energy, and photocatalytic activity. A lower band gap allows ZnO to absorb light more effectively, resulting in improved degradation performance. Among the samples, ZnO-DP10 shows the highest activity, confirming that higher extract concentration contributes to better photocatalytic efficiency under the conditions used in this study. However, the results should be interpreted within the scope of the experimental setup used, as variations in testing conditions may influence the observed performance. Overall, the findings highlight that controlling extract concentration is a simple and effective approach to enhance the degradation of methylene blue using ZnO nanoparticles.

Acknowledgment

This work was supported by Direktorat Riset, Teknologi, dan Pengabdian kepada Masyarakat Kementerian Pendidikan Tinggi, Sains, dan Teknologi through "Penelitian Dosen Pemula Perguruan Tinggi" (grant number 018/C3/DT.05.00/PL/2025)

References

- [1] J. Ge, Y. Zhang, Y.-J. Heo, and S.-J. Park, "Advanced design and synthesis of composite photocatalysts for the remediation of wastewater: A review," *Catalysts*, vol. 9, no. 2, p. 122, 2019.
- [2] N. Chaukura *et al.*, "Development and evaluation of a low-cost ceramic filter for the removal of methyl orange, hexavalent chromium, and *Escherichia coli* from water," *Materials Chemistry and Physics*, vol. 249, p. 122965, 2020.
- [3] B. Liu, A. Khan, K.-H. Kim, D. Kukkar, and M. Zhang, "The adsorptive removal of lead ions in aquatic media: Performance comparison between advanced functional materials and conventional materials," *Critical Reviews in Environmental Science and Technology*, vol. 50, no. 23, pp. 2441-2483, 2020.
- [4] B. Siripireddy and B. K. Mandal, "Facile green synthesis of zinc oxide nanoparticles by *Eucalyptus globulus* and their photocatalytic and antioxidant activity," *Advanced Powder Technology*, vol. 28, no. 3, pp. 785-797, 2017.
- [5] K. M. Lee, C. W. Lai, K. S. Ngai, and J. C. Juan, "Recent developments of zinc oxide based photocatalyst in water treatment technology: A review," *Water Research*, vol. 88, pp. 428-448, Jan. 2016.
- [6] A. Rafiq *et al.*, "Photocatalytic degradation of dyes using semiconductor photocatalysts to clean industrial water pollution," *Journal of Industrial and Engineering Chemistry*, vol. 97, pp. 111-128, 2021.
- [7] T. L. Yusuf, B. O. Orimolade, D. Masekela, B. Mamba, and N. Mabuba, "The application of photoelectrocatalysis in the degradation of rhodamine B in aqueous solutions: a review," *RSC advances*, vol. 12, no. 40, pp. 26176-26191, 2022.

- [8] S. A. Kumar, M. Jarvin, S. Sharma, A. Umar, S. S. R. Inbanathan, and N. P. Lalla, "Facile and green synthesis of MgO nanoparticles for the degradation of victoria blue dye under UV irradiation and their antibacterial activity," *ES Food and Agroforestry*, vol. 5, no. 12, pp. 14-19, 2021.
- [9] Y. Kaur, T. Jasrotia, R. Kumar, G. R. Chaudhary, and S. Chaudhary, "Adsorptive removal of eriochrome black T (EBT) dye by using surface active low cost zinc oxide nanoparticles: A comparative overview," *Chemosphere*, vol. 278, p. 130366, 2021.
- [10] H. Y. Samayoa-Oviedo, S. A. Mehnert, M. F. Espenship, M. R. Weigand, and J. Laskin, "Measurement of the speciation diagram of thymol blue using spectrophotometry," *Journal of Chemical Education*, vol. 100, no. 2, pp. 815-821, 2022.
- [11] Z. Kalaycıoğlu, B. Özüğür Uysal, Ö. Pekcan, and F. B. Erim, "Efficient Photocatalytic Degradation of Methylene Blue Dye from Aqueous Solution with Cerium Oxide Nanoparticles and Graphene Oxide-Doped Polyacrylamide," *ACS Omega*, vol. 8, no. 14, pp. 13004-13015, Apr. 2023.
- [12] P. O. Oladoye, T. O. Ajiboye, E. O. Omotola, and O. J. Oyewola, "Methylene blue dye: Toxicity and potential elimination technology from wastewater," *Results in Engineering*, vol. 16, p. 100678, 2022.
- [13] G. Crini and E. Lichtfouse, "Advantages and disadvantages of techniques used for wastewater treatment," *Environmental chemistry letters*, vol. 17, no. 1, pp. 145-155, 2019.
- [14] H. Sukmana, N. Bellahsen, F. Pantoja, and C. Hodur, "Adsorption and coagulation in wastewater treatment-Review," *Progress in Agricultural Engineering Sciences*, vol. 17, no. 1, pp. 49-68, 2021.
- [15] M. Beydaghdari, F. H. Saboor, A. Babapoor, and M. Asgari, "Recent progress in adsorptive removal of water pollutants by metal-organic frameworks," *ChemNanoMat*, vol. 8, no. 2, p. e202100400, 2022.
- [16] Z. Shayegan, C.-S. Lee, and F. Haghightat, "TiO₂ photocatalyst for removal of volatile organic compounds in gas phase-A review," *Chemical Engineering Journal*, vol. 334, pp. 2408-2439, 2018.
- [17] S. Abou Zeid and Y. Leprince-Wang, "Advancements in ZnO-based photocatalysts for water treatment: a comprehensive review," *Crystals*, vol. 14, no. 7, p. 611, 2024.
- [18] F. Zhang *et al.*, "Recent advances and applications of semiconductor photocatalytic technology," *Applied Sciences*, vol. 9, no. 12, p. 2489, 2019.
- [19] N. Kumar and A. Srivastava, "Faster photoresponse, enhanced photosensitivity and photoluminescence in nanocrystalline ZnO films suitably doped by Cd," *Journal of Alloys and Compounds*, vol. 706, pp. 438-446, Jun. 2017.
- [20] A. S. Abdelbaky, T. A. Abd El-Mageed, A. O. Babalghith, S. Selim, and A. M. H. A. Mohamed, "Green Synthesis and Characterization of ZnO Nanoparticles Using Pelargonium odoratissimum (L.) Aqueous Leaf Extract and Their Antioxidant, Antibacterial and Anti-inflammatory Activities," *Antioxidants*, vol. 11, no. 8, p. 1444, Jul. 2022.
- [21] S. Fakhari, M. Jamzad, and H. Kabiri Fard, "Green synthesis of zinc oxide nanoparticles: a comparison," *Green Chemistry Letters and Reviews*, vol. 12, no. 1, pp. 19-24, Jan. 2019.
- [22] R. Hazrati Saadabadi, F. Shariatmadar Tehrani, Z. Sabouri, and M. Darroudi, "Photocatalytic activity and anticancer properties of green synthesized ZnO-MgO-

- Mn₂O₃ nanocomposite via *Ocimum basilicum* L. seed extract," *Sci Rep*, vol. 14, no. 1, p. 29812, Nov. 2024.
- [23] C. Mallikarjunaswamy, V. Lakshmi Ranganatha, R. Ramu, Udayabhanu, and G. Nagaraju, "Facile microwave-assisted green synthesis of ZnO nanoparticles: application to photodegradation, antibacterial and antioxidant," *Journal of Materials Science: Materials in Electronics*, vol. 31, no. 2, pp. 1004–1021, Jan. 2020.
- [24] K. Subham, J. Kaur, M. Chakroborty, and S. G. Manuel, "Green synthesis of zinc oxide nanoparticles using the extracts of *Calotropis gigantea*, *Foeniculum Vulgare* and *Murraya Koenigii* and their Antimicrobial Properties," *Journal of Advanced Scientific Research*, vol. 11, no. 03, pp. 183–188, 2020.
- [25] D. E. Kwabena and A. E. Aquisman, "Morphology of green synthesized ZnO nanoparticles using low temperature hydrothermal technique from aqueous *Carica papaya* extract," *Nanosci. Nanotechnol.*, vol. 9, no. 1, pp. 29–36, 2019.
- [26] M. F. S. Hermandy, M. Z. M. Yusoff, M. S. Yahya, and M. R. Awal, "The green synthesis of nanoparticle zinc oxide (ZnO) using aloe vera leaf extract: structural and optical characterization reviews," *International Journal*, vol. 8, no. 10, pp. 6896–6902, 2020.
- [27] H. M. Albert and A. Gonsago, "Green synthesis of Zinc oxide nanoparticles using *Solanum nigrum* leaf extract and overview of their antibacterial activities," *Journal of Advanced Scientific Research*, vol. 14, no. 05, pp. 26–30, 2023.
- [28] T. B. Vidovix, H. B. Quesada, E. F. D. Januário, R. Bergamasco, and A. M. S. Vieira, "Green synthesis of copper oxide nanoparticles using *Punica granatum* leaf extract applied to the removal of methylene blue," *Materials Letters*, vol. 257, p. 126685, 2019.
- [29] K. D. Dejen, E. A. Zereffa, H. A. Murthy, and A. Merga, "Synthesis of ZnO and ZnO/PVA nanocomposite using aqueous *Moringa oleifera* leaf extract template: antibacterial and electrochemical activities," *Rev. Adv. Mater. Sci.*, vol. 59, no. 1, pp. 464–476, 2020.
- [30] K. D. Dejen, E. A. Zereffa, H. A. Murthy, and A. Merga, "Synthesis of ZnO and ZnO/PVA nanocomposite using aqueous *Moringa oleifera* leaf extract template: antibacterial and electrochemical activities," *Rev. Adv. Mater. Sci.*, vol. 59, no. 1, pp. 464–476, 2020.
- [31] F. Zahara, D. Yuniharni, and I. Arziqni, "Optimasi Ekstraksi Flavonoid Dari Daun Pisang Kepok (*Musa Paradisiaca* L) Menggunakan Microwave-Assisted Extraction (Mae)," *Jurnal Teknologi Kimia Unimal*, vol. 12, no. 2, p. 190, 2023.
- [32] F. N. Alharbi, Z. M. Abaker, and S. Z. A. Makawi, "Phytochemical substances – mediated synthesis of zinc oxide nanoparticles (ZnO NPS)," *Inorganics*, vol. 11, no. 8, p. 328, 2023.
- [33] Y. C. Khefanny, Charlena, and S. Sugiarti, "Synthesis and Characterization of ZnO/Cellulose Acetate Composite and its Activity as Antibacterial Agent," *sci. technol. indones.*, vol. 9, no. 2, pp. 215–223, Apr. 2024, doi: 10.26554/sti.2024.9.2.215-223.
- [34] Y. E. Agustin and K. S. Padmawijaya, "Effect of glycerol and zinc oxide addition on antibacterial activity of biodegradable bioplastics from chitosan-kepok banana peel starch," *IOP Conference Series: Materials Science and Engineering*, vol. 223, no. 1, p. 012046, Jul. 2017.

- [35] S. Marfu'ah *et al.*, "Green Synthesis of ZnO Nanoparticles by Using Banana Peel Extract as Capping agent and Its Bacterial Activity," *IOP Conference Series: Materials Science and Engineering*, vol. 833, no. 1, p. 012076, May 2020.
- [36] A. Setiawan, L. R. Dianti, N. E. Mayangsari, D. R. Widiana, and D. Dermawan, "Removal of methylene blue using heterogeneous Fenton process with Fe impregnated kepok banana (*Musa acuminata* L.) peel activated carbon as catalyst," *Inorganic Chemistry Communications*, vol. 152, p. 110715, 2023.
- [37] C. A. Soto-Robles *et al.*, "Study on the effect of the concentration of Hibiscus sabdariffa extract on the green synthesis of ZnO nanoparticles," *Results in Physics*, vol. 15, p. 102807, Dec. 2019.
- [38] S. Musić, Đ. Dragčević, S. Popović, and M. Ivanda, "Precipitation of ZnO particles and their properties," *Materials Letters*, vol. 59, no. 19–20, pp. 2388–2393, Aug. 2005.
- [39] T. Gur, I. Meydan, H. Seckin, M. Bekmezci, and F. Sen, "Green synthesis, characterization and bioactivity of biogenic zinc oxide nanoparticles," *Environmental Research*, vol. 204, p. 111897, 2022.
- [40] P. Ramesh, K. Saravanan, P. Manogar, J. Johnson, E. Vinoth, and M. Mayakannan, "Green synthesis and characterization of biocompatible zinc oxide nanoparticles and evaluation of its antibacterial potential," *Sensing and Bio-Sensing Research*, vol. 31, p. 100399, 2021.
- [41] A. M. Pillai *et al.*, "Green synthesis and characterization of zinc oxide nanoparticles with antibacterial and antifungal activity," *Journal of Molecular Structure*, vol. 1211, p. 128107, 2020.
- [42] T. Nishinaga, *Handbook of crystal growth: fundamentals*. Elsevier, 2014.
- [43] R. S. Prabhu, R. Priyanka, M. Vijay, and G. K. Vikashini, "Field emission scanning electron microscopy (FESEM) with a very big future in pharmaceutical research," *International Journal of Pharmacy and Biological Sciences*, vol. 11, no. 2, pp. 183–187, 2021.
- [44] J. Kadam, P. Dhawal, S. Barve, and S. Kakodkar, "Green synthesis of silver nanoparticles using cauliflower waste and their multifaceted applications in photocatalytic degradation of methylene blue dye and Hg²⁺ biosensing," *SN Applied Sciences*, vol. 2, no. 4, p. 738, 2020.
- [45] X. Zhu *et al.*, "Fabrication, characterization and high photocatalytic activity of Ag-ZnO heterojunctions under UV-visible light," *RSC advances*, vol. 11, no. 44, pp. 27257–27266, 2021.
- [46] M. Ahmad *et al.*, "Enhanced photocatalytic activity of Ce-doped ZnO nanopowders synthesized by combustion method," *Journal of rare earths*, vol. 33, no. 3, pp. 255–262, 2015.
- [47] R. E. Aderne *et al.*, "On the energy gap determination of organic optoelectronic materials: the case of porphyrin derivatives," *Materials Advances*, vol. 3, no. 3, pp. 1791–1803, 2022.
- [48] A. R. Zanatta, "Revisiting the optical bandgap of semiconductors and the proposal of a unified methodology to its determination," *Scientific reports*, vol. 9, no. 1, p. 11225, 2019.
- [49] S. S. Abdullahi, S. Güner, Y. Koseoglu, I. M. Musa, B. I. Adamu, and M. I. Abdulhamid, "Simple method for the determination of band gap of a nanopowdered sample using Kubelka Munk theory," *NAMP J*, vol. 35, pp. 241–246, 2016.

- [50] M. R. Parra and F. Z. Haque, "Aqueous chemical route synthesis and the effect of calcination temperature on the structural and optical properties of ZnO nanoparticles," *Journal of Materials Research and Technology*, vol. 3, no. 4, pp. 363–369, 2014.
- [51] A. Alnehia, A.-B. Al-Odayni, A. Al-Sharabi, A. H. Al-Hammadi, and W. S. Saeed, "Pomegranate peel extract-mediated green synthesis of ZnO-NPs: extract concentration-dependent structure, optical, and antibacterial activity," *Journal of Chemistry*, vol. 2022, no. 1, p. 9647793, 2022.
- [52] X. Chen, H. Zhang, J. Li, and L. Chen, "Analysis of chemical compounds of pomegranate peel polyphenols and their antibacterial action against *Ralstonia solanacearum*," *South African Journal of Botany*, vol. 140, pp. 4–10, 2021.
- [53] S. Saleem *et al.*, "Modification in structural, optical, morphological, and electrical properties of zinc oxide (ZnO) nanoparticles (NPs) by metal (Ni, Co) dopants for electronic device applications," *Arabian Journal of Chemistry*, vol. 15, no. 1, p. 103518, 2022.
- [54] U. L. Ifeanyichukwu, O. E. Fayemi, and C. N. Ateba, "Green synthesis of zinc oxide nanoparticles from pomegranate (*Punica granatum*) extracts and characterization of their antibacterial activity," *Molecules*, vol. 25, no. 19, p. 4521, 2020.
- [55] S. A. Akintelu and A. S. Folorunso, "A review on green synthesis of zinc oxide nanoparticles using plant extracts and its biomedical applications," *BioNanoScience*, vol. 10, no. 4, pp. 848–863, 2020.
- [56] A. M. Al-Baradi *et al.*, "Structural and optical characteristic features of RF sputtered CdS/ZnO thin films," *Chinese Physics B*, vol. 29, no. 8, p. 080702, 2020.
- [57] M.-A. Gatou, N. Lagopati, I.-A. Vagena, M. Gazouli, and E. A. Pavlatou, "ZnO nanoparticles from different precursors and their photocatalytic potential for biomedical use," *Nanomaterials*, vol. 13, no. 1, p. 122, 2022.
- [58] K. Raja, P. S. Ramesh, and D. Geetha, "Structural, FTIR and photoluminescence studies of Fe doped ZnO nanopowder by co-precipitation method," *Spectrochimica acta part A: molecular and biomolecular spectroscopy*, vol. 131, pp. 183–188, 2014.
- [59] V. Hoseinpour, M. Souiri, N. Ghaemi, and A. Shakeri, "Optimization of green synthesis of ZnO nanoparticles by *Dittrichia graveolens* (L.) aqueous extract," *Health Biotechnol. Biopharma*, vol. 1, no. 2, pp. 39–49, 2017.
- [60] D. Mutukwa, R. T. Taziwa, and L. Khotseng, "A Review of Plant-Mediated ZnO Nanoparticles for Photodegradation and Antibacterial Applications," *Nanomaterials*, vol. 14, no. 14, p. 1182, Jul. 2024.
- [61] H. M. Rasheed, K. Aroosh, D. Meng, X. Ruan, M. Akhter, and X. Cui, "A review on modified ZnO to address environmental challenges through photocatalysis: Photodegradation of organic pollutants," *Materials Today Energy*, vol. 48, p. 101774, Mar. 2025.
- [62] J. Osuntokun, D. C. Onwudiwe, and E. E. Ebenso, "Green synthesis of ZnO nanoparticles using aqueous *Brassica oleracea* L. var. *italica* and the photocatalytic activity," *Green Chemistry Letters and Reviews*, vol. 12, no. 4, pp. 444–457, Oct. 2019.
- [63] T. C. Raganata, H. Aritonang, and E. Suryanto, "SINTESIS FOTOKATALIS NANOPARTIKEL ZnO UNTUK MENDEGRADASI ZAT WARNA METHYLENE BLUE," *chemprog*, vol. 12, no. 2, Jan. 2020.